$$H_{cd}=H_{ef}=g^2\beta^2b^{\frac{3}{2}}L^2K^2\pi^{-\frac{1}{2}}\{1/15+e^{-\Delta}S_1(4\Delta)\},$$
$$H_{ca}=H_{cb}=H_{ce}=H_{cf}=0,$$
$$H_{ad}=H_{bd}=H_{ae}=H_{be}=H_{af}=H_{bf}=H_{de}=H_{df}=0,$$
$$H_{cg}=-H_{ch}=-H_{ci}=2^{-\frac{1}{2}}ReH_{cE}=g^2\beta^2b^{\frac{3}{2}}JKLM(2\pi)^{-\frac{1}{2}}e^{-\Delta}$$
$$\times\{(e^{\Delta}/15)[\Delta+B\Delta^{\frac{1}{2}}-BE+\tfrac{1}{2}-5e^{-\Delta}/14]$$
$$-(B+\Delta^{\frac{1}{2}})(E+\Delta^{\frac{1}{2}})S_1(4\Delta)$$
$$-4[\Delta+\Delta^{\frac{1}{2}}(2B-E)]e^{\Delta/4}S_1(\Delta)-\tfrac{1}{2}S_2(4\Delta)$$
$$+\tfrac{1}{4}\Delta^{-\frac{3}{2}}(3\Delta^{\frac{1}{2}}+2B+E)S_3(4\Delta)$$
$$+4\Delta^{-\frac{3}{2}}(\Delta^{\frac{1}{2}}+2B-E)e^{\Delta/4}S_3(\Delta)+\tfrac{1}{8}\Delta^{-2}S_4(4\Delta)\}.$$

In these,

$$S_2(x)=\sum_{n=1}^{\infty}\frac{1}{1\cdot3\cdot5\cdots(2n+3)}\left(\frac{x}{2}\right)^n,$$

$$S_3(x)=\left(\frac{x}{2}\right)\sum_{n=1}^{\infty}\frac{(2n)(2n-1)}{1\cdot3\cdot5\cdots(2n+5)}\left(\frac{x}{2}\right)^n,$$

$$S_4(x)=\left(\frac{x}{2}\right)\sum_{n=1}^{\infty}\frac{2n(2n-1)^2}{1\cdot3\cdot5\cdots(2n+5)}\left(\frac{x}{2}\right)^n,$$

and the constants B, E, J, L, and M are as defined by Meckler.[2] In evaluating H_{cg}, the terms in ϕ_0 and χ_0 giving orthogonality to the $1s$ orbitals have been dropped as negligible to allow integration by our artifice (which requires a common Gaussian factor for all orbitals). We note that all of the elements have the same sort of dependence on $b^{\frac{3}{2}}$ and $bR^2=\Delta$, the Δ dependence turning out to be rather slight.

PHYSICAL REVIEW VOLUME 97, NUMBER 4 FEBRUARY 15, 1955

Interaction of Molecular Oxygen with a Magnetic Field*

M. TINKHAM† AND M. W. P. STRANDBERG
Department of Physics and Research Laboratory of Electronics, Massachusetts Institute of Technology, Cambridge, Massachusetts
(Received June 9, 1954)

The dominant interaction of O_2 with a magnetic field is through the electronic spin magnetic moment. However, a precise comparison with experiment of the results of calculating the microwave paramagnetic spectrum, assuming only this interaction, shows a systematic discrepancy. This discrepancy is removed by introducing two corrections. The larger (approximately 0.1 percent, or 7 gauss) is a correction for the second-order electronic orbital moment coupled in by the spin-orbit energy. Its magnitude is proportional to the second-order term μ'' in the spin-rotation coupling constant. The smaller (approximately 1 gauss) is a correction for the rotation-induced magnetic moment of the molecule. Since the dependence of this contribution on quantum numbers is quite unique, this coefficient can also be determined by fitting the magnetic spectrum. A total of 120 X-band and 78 S-band lines were observed. The complete corrections have been made on 26 lines with a mean residual error of roughly 0.5 Mc/sec. This excellent agreement confirms the anomalous electronic moment to 60 parts per million (ppm) and also confirms the validity of the Zeeman-effect theory.

A new result is the rotational magnetic moment of -0.25 ± 0.05 nuclear magnetons per quantum of rotation. Knowledge of this moment allows the electronic contribution to the effective moment of inertia to be determined. Making this correction of 65 ppm, and using the latest fitting of the universal atomic constants, the equilibrium internuclear distance is recomputed to be $R_e=1.20741\pm0.00002$ A. We can also deduce that the magnitude of λ'', the second-order spin-orbit contribution to the coupling of the spin to the figure axis, is 465 ± 50 Mc/sec, or less than one percent of the total coupling constant λ.

Theoretical intensities of a number of the microwave transitions are calculated and successfully compared with experiment over a range of 100 to 1 in magnitude. It turns out that $\Delta M=0$ transitions are over a hundred times weaker than the $\Delta M=\pm1$ transitions and thus are too weak to observe. Also, J breaks down as a quantum number in the presence of a magnetic field. This allows $\Delta J=\pm2$ transitions to comprise roughly half of all lines observed.

IN a previous paper[1] (referred to as TSI), we gave a rather complete and precise treatment of the eigenvalues, eigenvectors, and transition intensities of the oxygen molecule in field-free space. Using this work as a foundation, we now give a similarly complete and precise treatment of the perturbations produced by a magnetic field. The dominant interaction will, of course, be that between the electronic spin magnetic moment and the external field; namely,

$$\mathcal{H}_{ms}=-g_s{}^e\beta\mathbf{S}\cdot\mathbf{H}. \quad (1)$$

Accordingly, the effects of this perturbation on the eigenvalues and eigenvectors is first determined to high accuracy. It is then found necessary to introduce the small effects of spin-orbit coupling and rotation-induced moments as additional perturbations to fit the precise experimental data. The fitting evaluates certain sums of matrix elements which are important in interpreting the field-free parameters λ and μ. Incidentally, the fit may also be considered to confirm the theoretical anomalous moment of the electron to ±60 parts per million (ppm). Selection rules and intensities will also be discussed and compared with experiment. It turns out that $\Delta M=\pm1$, 0 transitions are allowed, but the $\Delta M=0$ lines are at least 100 times weaker than the $\Delta M=\pm1$.

* This work was supported in part by the Signal Corps, the Air Materiel Command, and the Office of Naval Research.
† National Science Foundation Predoctoral Fellow.
[1] M. Tinkham and M. W. P. Strandberg, preceding paper [Phys. Rev. **97**, 937 (1955)].

I. INTERACTION OF ELECTRONIC SPIN WITH EXTERNAL FIELD

A. Eigenvalues

If we define the direction of the external field to be the Z direction, then the matrix of our perturbed Hamiltonian is that of[2]

$$\mathcal{H}=\mathcal{H}_0+\mathcal{H}_{ms}=\mathcal{H}_0-g_s^e\beta HS_Z, \tag{2}$$

where $g_s^e=-2.00229$, β is the Bohr magneton, H is the magnitude of the applied field, and $\mathcal{H}_0$ is the field-free Hamiltonian treated in TSI. Matrix elements of S_Z in the basis which diagonalizes the field-free problem have been given previously [TSI Eq. (60) and Table VIII]. Noting that there are $\Delta K=\pm2$, 0 as well as $\Delta J=\pm1$, 0 elements, we find that $\mathcal{H}_{ms}$ does not factor into smaller submatrices which can be diagonalized exactly. If O_2 were a rigorous example of Hund's case (b) in which K is a good quantum number, there would be no $\Delta K=\pm2$ elements and the problem would be factored into 3×3 submatrices, one for each value of K. This factored form is the starting point taken for further approximations in the treatment of Schmid, Budó, and Zemplén,[3] but is completely inadequate for our purposes. Although it is a better approximation, Henry's method[4] is also too inaccurate.

The matrix of the complete Hamiltonian has the form:

$$\begin{array}{c|cccccccccc}
 & & & & & 0 & & 0 & & 0 \\
 & & x & x & 0 & 0 & 0 & & & \\
K-2 & & x & x & x & x & 0 & 0 & 0 & \\
 & & 0 & x & x & x & x & 0 & & \\
 & & & & & & & & & \\
 & & 0 & x & x & x & x & 0 & 0 & 0 \\
K & 0 & 0 & 0 & x & x & x & x & 0 & 0 & 0 \\
 & & 0 & 0 & 0 & 0 & x & x & x & x & 0 \\
 & & & & & & & & & \\
 & & & & & 0 & x & x & x & x & 0 \\
K+2 & 0 & & 0 & & 0 & 0 & x & x & x & x \\
 & & & & & 0 & 0 & 0 & 0 & x & x \\
 & & & & & & & & & & \\
 & 0 & & 0 & & 0 & & & & &
\end{array}. \tag{3}$$

Since the energy separation between rotational levels is large compared to the magnetic perturbation, the dominant effect will come from the elements diagonal in K. The effects of elements which are off-diagonal in K may be reduced to the diagonal (in K) by the Van Vleck transformation.[5,6] The resulting $(J|\mathcal{H}|J')$ elements for the effective 3×3 Hamiltonian matrix for the Kth rotational level are:

$$H_{11}=(K-1|\mathcal{H}|K-1)=-\nu_-(K)-g(K,K-1)M\beta H$$
$$+\left\{\frac{D_{K-1}^2[(K-1)^2-M^2]}{(4K-2)B-\nu_-(K)}+\frac{h_{K-1}^2M^2}{(4K-2)B+[g(K-2,K-1)-g(K,K-1)]\beta HM}\right\}(g_s^e)^2\beta^2H^2,$$

$$H_{22}=(K|\mathcal{H}|K)=-g(K,K)M\beta H+\frac{A_{K-1}^2(K^2-M^2)(g_s^e)^2\beta^2H^2}{(4K-2)B}-\frac{D_{K+1}^2[(K+1)^2-M^2](g_s^e)^2\beta^2H^2}{(4K+6)B},$$

$$H_{33}=(K+1|\mathcal{H}|K+1)=-\nu_+(K)-g(K,K+1)M\beta H$$
$$-\left\{\frac{h_{K+1}^2M^2}{(4K+6)B-[g(K+2,K+1)-g(K,K+1)]M\beta H}+\frac{A_{K+1}^2[(K+2)^2-M^2]}{(4K+6)B+\nu_+(K)}\right\}(g_s^e)^2\beta^2H^2, \tag{4}$$

$$H_{12}=(K|\mathcal{H}|K-1)=-C_{K-1}(K^2-M^2)^{\frac{1}{2}}g_s^e\beta H+\frac{h_{K-1}A_{K-1}M(K^2-M^2)^{\frac{1}{2}}(g_s^e)^2\beta^2H^2}{(4K-2)B},$$

$$H_{23}=(K|\mathcal{H}|K+1)=-B_{K+1}[(K+1)^2-M^2]^{\frac{1}{2}}g_s^e\beta H-\frac{h_{K+1}D_{K+1}M[(K+1)^2-M^2]^{\frac{1}{2}}(g_s^e)^2\beta^2H^2}{(4K+6)B},$$

$$H_{13}=(K-1|\mathcal{H}|K+1)=0.$$

[2] Our systematic notation is to use superscripts e and n to distinguish electronic and nuclear contributions, and we use subscripts s, l, r to distinguish spin, spin-orbit, and rotation. All g-factors have the appropriate sign so that $\boldsymbol{\mu}=g\beta\mathbf{J}$; for example, that of the electron is a negative number. To conform to conventional usage we denote the magnetic field by H but give numerical values in gauss, the units of magnetic induction.

[3] Schmid, Budó, and Zemplén, Z. Physik **103**, 250 (1936).

[4] A. F. Henry, Phys. Rev. **80**, 396 (1950).

[5] E. C. Kemble, *Fundamental Principles of Quantum Mechanics* (McGraw-Hill Book Company, Inc., New York, 1939).

[6] To get sufficient accuracy here, we use some energy denominators corrected to first order. This procedure is readily justified if the elements are derived by the method of continued fraction reduction. The error remaining from the reduction is then definitely less than 1 Mc/sec for all cases of interest.

In the diagonal elements we have suppressed the common term $BK(K+1)$. The secular equation is

$$\begin{vmatrix} H_{11}-E & H_{12} & 0 \\ H_{12} & H_{22}-E & H_{23} \\ 0 & H_{23} & H_{33}-E \end{vmatrix}=0. \tag{5}$$

The complex dependence of the elements on parameters makes a straight numerical solution the most attractive procedure. For this purpose, the continued fraction forms are most useful. They are

$$E_1=H_{11}-\cfrac{H_{12}^2}{H_{22}-E_1-H_{23}^2/(H_{33}-E_1)}$$

and (6)

$$E_2=H_{22}+\cfrac{H_{23}^2}{E_2-H_{33}}+\cfrac{H_{12}^2}{E_2-H_{11}}.$$

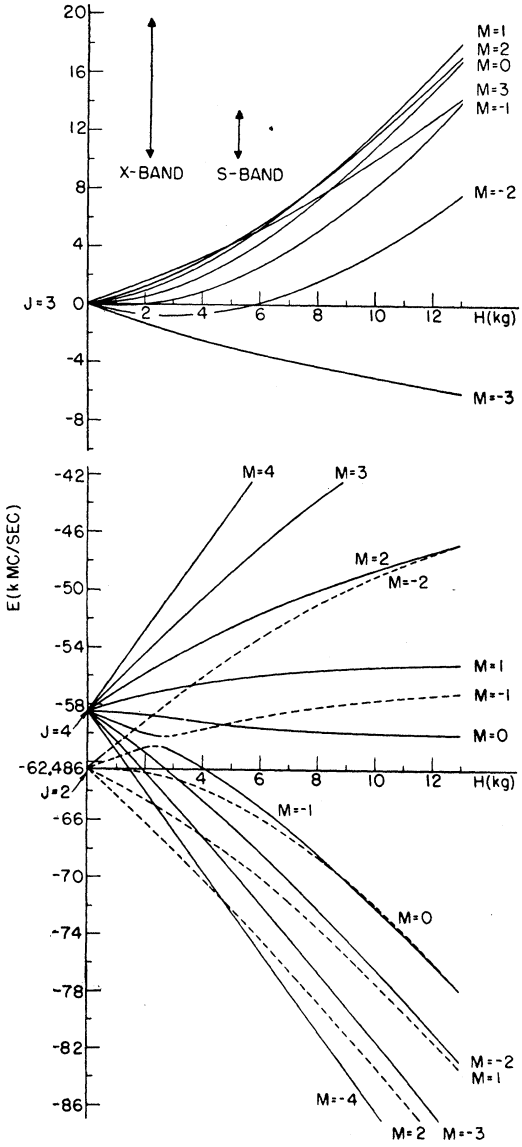

FIG. 1. Magnetic splitting of the $K=3$ energy levels.

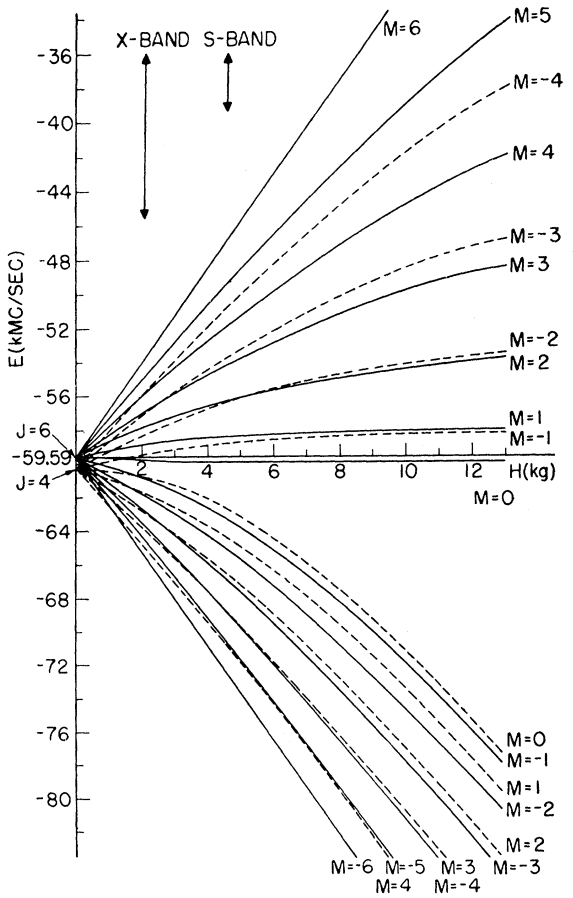

Fig. 2. Magnetic splitting of the $K=5$; $J=4,6$ energy levels.

The expression for E_3 is obtained from that for E_1 by interchanging the subscripts 1 and 3. These equations are exact equivalents of (5) and not a perturbation approximation. If the roots are well separated, convergence to the desired root on iteration is rapid. If two roots are close together, convergence is slow.

The roots E_1, E_2, and E_3 have been evaluated to ± 10 Mc/sec at $H=4$, 8, and 12 kilogauss for most M states for $K \leqslant 13$. The results have been plotted against H by graphical interpolation.[7] Some examples are shown in Figs. 1 and 2. The small g-factors for $J=K$ states [roughly $-2/K(K+1)$] make their splittings very small, only three cases being as wide as 9400 Mc/sec for fields under 12 kilogauss. Thus most attention can be concentrated on the $J=K\pm 1$ levels. For $K \geqslant 3$, the families of curves are all quite similar. (The $K=1$ curves are simpler, since the $J=0$ and $J=2$ levels are widely separated.) For H less than a few hundred gauss, the splittings closely resemble the linear Zeeman splitting predicted by the field-free g-factors (TSI, Table VIII). At very high fields the Paschen-Back effect

[7] The numerical results and more graphs are given in the Ph.D. thesis of M. Tinkham, Massachusetts Institute of Technology, 1954 (unpublished).

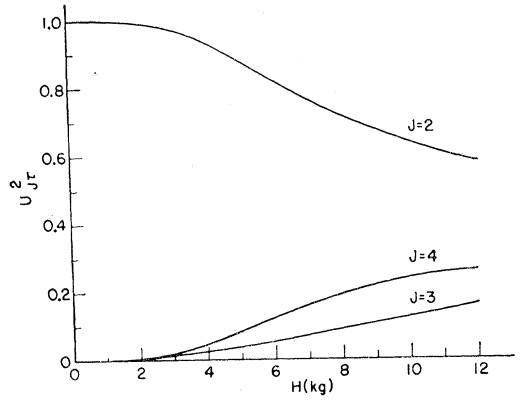

FIG. 3. Mixing coefficients of the J components in the $K=3$, $M=0$ state of lowest energy.

sets in and we approach the limiting case of a completely decoupled spin. Then there must be $(2K+1)$ levels corresponding to each of $M_S=\pm 1$, 0. That this tendency is observed becomes clear if we note by inspection of the graphs that all the $(2K+1)$ levels from $J=K$ are asymptotically going to $M_S=1$ except the $M=-K$ level, which goes to $M_S=0$. Similarly the $(4K+2)$ sublevels from $J=K\pm 1$ provide $(2K+1)$ of $M_S=-1$, $2K$ of $M_S=0$, and the single $M=K+1$ sublevel of $M_S=1$. These numbers check the proper limiting behavior. Even at fields as low as 8 kilogauss there is a marked tendency for the set of $M_S=-1$ levels to split off into a bundle of nearly parallel lines of slope equal to $g_s{}^e\beta$. In the intermediate region, which is of most interest, we find the characteristic repulsion of levels of the same M and the accompanying strong curvature.

From these curves the approximate values of H for a given resonant frequency ν (energy level separation) may be found to an accuracy of about ± 100 gauss. This is close enough to identify many lines of the spectrum if full use is made of experimental information on K and ΔM. However, to give a secure identification and to check the theory in detail, each line must be calculated individually.

This calculation was made by computing the position (to ± 0.5 Mc/sec) of both levels involved in the transition for two values of H separated by 200 gauss and centered about the approximately correct field, determined graphically. If the transition frequency is then expressed as

$$\nu(H)=\nu(H_0)+(d\nu/dH)(H-H_0), \tag{7}$$

the two calculated points fix $\nu(H_0)$ and $d\nu/dH$. This formula allows the calculated resonant field for any given experimental frequency to be determined to approximately ± 0.5 gauss, since the curvature can be shown to be small over a region of a hundred gauss. The value of $d\nu/dH$ is also necessary to interpret linewidth measurements at constant frequency and to make corrections for various perturbations to be considered later. The values of H for the experimental ν, and the value of $d\nu/dH$ at that H, are given for many lines of the spectrum in Tables I and III.

B. Eigenvectors

From the form of (3) it is evident that only M is a good quantum number in the presence of a magnetic field, since, in principle, *all* J's and K's are mixed. However, the principal mixing is between the three J values corresponding to one K. The admixture of other K states is small and could be treated by perturbation theory. In the worst case this amounts to only about a one percent mixing amplitude even at 10 kilogauss. Since this is too small to have any serious effect on any of our subsequent calculations, we neglect these effects and only compute the transformation between the field-free and final eigenfunctions within a given K rotational triplet.

This transformation matrix is made up of the eigenvectors of the matrix equation corresponding to (5), and it is written

$$U_K=\begin{array}{c} \\ J=K-1 \\ J=K \\ J=K+1 \end{array}\begin{array}{c} \begin{array}{ccc} \tau=1 & \tau=2 & \tau=3 \end{array} \\ \begin{bmatrix} U_{11} & U_{12} & U_{13} \\ U_{21} & U_{22} & U_{23} \\ U_{31} & U_{32} & U_{33} \end{bmatrix} \end{array}. \tag{8}$$

In this, τ denotes the new eigenfunctions but signifies no constant of the motion except the energy. The elements $U_{J\tau}$ are defined by

$$\frac{U_{2\tau}}{U_{1\tau}}=\frac{E_\tau-H_{11}}{H_{12}} \qquad \frac{U_{3\tau}}{U_{2\tau}}=\frac{H_{23}}{E_\tau-H_{33}} \tag{9}$$

and normalization.

Examples plotted in Figs. 3 and 4 show two typical cases. In Fig. 3 we see the distortion of the $K=3$, $M=0$ state which starts as $J=2$ at zero field. At a field of 6 kilogauss the amplitude of $J=4$ has risen to 0.35, and that of $J=3$ has risen to 0.24. These figures show the substantial breakdown of J as a quantum number

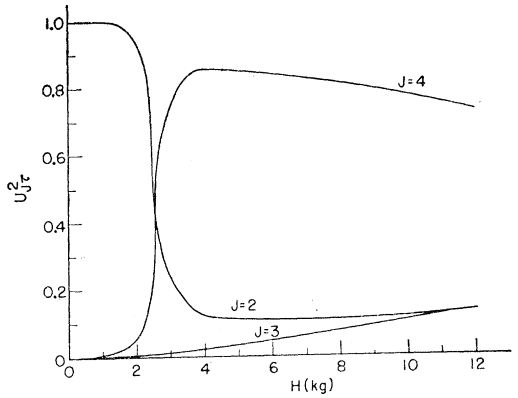

FIG. 4. Mixing coefficients of the J components in the $K=3$, $M=-1$ state of lowest energy.

under a magnetic field. This makes all $\Delta M=\pm 1, 0$ transitions "allowed," regardless of the principal or original value of J, provided the field is moderately strong. We will later see that the majority of the observed X-band transitions are of this field-allowed type. Figure 4 shows the more unusual case of two levels which attempt to cross each other but, instead, repel. At the point of closest approach the J's are completely mixed, and as the levels move apart again, the dominant J's are found to have interchanged. Since the strong mixing dies out rapidly, there is seldom any doubt as to which J is dominant in an eigenstate for a given field. We will use J in this sense throughout the paper rather than use the less suggestive τ notation introduced for the purpose of setting up the transformations U. The correct sense of J will always be clear from the context.

Numerical values for the transformation coefficients for a number of cases required in later parts of the calculation are given in Table VII. Inspection of this table shows how universal is the large degree of mixing.

II. CORRECTIONS FOR ROTATIONAL MAGNETIC MOMENT AND ELECTRONIC ORBITAL MAGNETISM

When the results of the calculations of Sec. I are compared with experiment (Tables I and III), a systematic discrepancy of the order 0.1 percent is obvious. Since this was far beyond the expected error of either theory or experiment, it was assumed to be caused by neglect of these corrections. When the corrections treated in this section are made, the agreement is within the accuracy of the experiment and calculations, namely of the order ± 50 ppm.

The straightforward and universally sound method of handling perturbative terms of this sort is simply to write down all matrix components of the energy in a convenient basis and then to eliminate the elements which are off-diagonal in electronic quantum numbers by the Van Vleck transformation.[5] For a case as simple as the diatomic molecule which we treat, however, the same results can be obtained without complication by using a shortcut method which gives a much clearer picture of the physical nature of the interactions. This second approach is followed here. Either method yields an effective Hamiltonian matrix involving fine structure quantum numbers only. The lowest-order contributions to the energy are then found by application of the transformation (within the fine structure levels) which diagonalizes the Hamiltonian $\mathcal{H}_0+\mathcal{H}_{ms}$.

In TSI we noted that the spin-orbit coupling and the rotation-electronic interaction mixed π states into the Σ electronic orbital state as follows:

$$\psi_\Sigma=\psi_\Sigma{}^0-\sum_{n=\pi}\sum_{g'=x,y}\frac{(n|AL_{g'}|0)S_{g'}-(n|2BL_{g'}|0)\mathfrak{R}_{g'}}{E_n-E_0}\psi_n{}^0. \tag{10}$$

The first-order electronic orbital angular momentum along the gth gyrating axis is then seen to be

$$\begin{aligned}L_g&=-\sum_{n,g'}\frac{(0|L_g|n)(n|AL_{g'}|0)S_{g'}+\text{comp. conj.}}{E_n-E_0}\\&\quad+\sum_{n,g'}\frac{(0|L_g|n)(n|2BL_{g'}|0)\mathfrak{R}_{g'}+\text{comp. conj.}}{E_n-E_0}\\&=-(g_l{}^eS_g+g_r{}^e\mathfrak{R}_g)(1-\delta_{g,z}),\end{aligned} \tag{11}$$

where

$$\begin{aligned}g_l{}^e&=2\,\mathrm{Re}\sum_n\frac{(0|L_x|n)(n|AL_x|0)}{E_n-E_0}\\ \text{and}\\ g_r{}^e&=-4\,\mathrm{Re}\sum_n\frac{(0|L_x|n)(n|BL_x|0)}{E_n-E_0}.\end{aligned} \tag{12}$$

In making this reduction we have used the facts that with axial symmetry the elements of L_x and L_y differ only by a phase of $\pm i$ [TSI, Eq. (26)] and that elements of L_z vanish for a Σ state. In the general case of lower symmetry the g's are not just diagonal tensors, but have the structure $(g_r{}^e)_{gg'}$, for example. Then L_g would be a sum of terms over g'. The general case of rotation-induced moments has been treated in detail by Eshbach and Strandberg.[8]

To obtain the interaction of this electronic orbital angular momentum with the external field, we project it onto the space-fixed Z-axis by using the direction cosine[9] matrix elements Φ_{Zg}:

$$L_Z=\sum_g\Phi_{Zg}L_g. \tag{13}$$

For our case, the matrix elements of this product operator which are diagonal in electronic quantum numbers between total state functions whose electronic part is (10) may be shown to be the same as those obtained by simply taking the product of the diagonal elements of L_g given in (11) and the elements of Φ_{Zg} for the case $\Lambda=0$. These Φ_{Zg} elements are the same as those used[9] in TSI to project S_g onto Z. Combining (11) and (13),

$$\begin{aligned}L_Z&=-g_l{}^e\sum_{g=x,y}\Phi_{Zg}S_g-g_r{}^e\sum_{g=x,y,z}\Phi_{Zg}\mathfrak{R}_g\\&=-g_l{}^e\sum_{g=x,y}\Phi_{Zg}S_g-g_r{}^e\mathfrak{R}_Z.\end{aligned} \tag{14}$$

The second sum may be extended to include $g=z$ because $\mathfrak{R}_z$ is zero. This is more convenient, since it gives rise to the simple expression $\mathfrak{R}_Z$. Noting that S_x and S_y are purely off-diagonal in Σ, whereas S_z is

[8] J. R. Eshbach and M. W. P. Strandberg, Phys. Rev. **85**, 24 (1952).

[9] See TSI, Table VI.

purely diagonal, we can write (14) as[10]

$$(JM\Sigma|L_Z|J'M\Sigma')=-g_r{}^e(JM\Sigma|\mathfrak{R}_Z|J'M\Sigma') -(1-\delta_{\Sigma,\Sigma'})g_l{}^e(JM\Sigma|S_Z|J'M\Sigma'). \quad (15)$$

Before computing the effect of this electronic orbital angular momentum on the magnetic energy, let us note that elementary considerations show that the magnetic moment of the rotating nuclei in a homonuclear diatomic molecule is simply

$$\mathfrak{y}_r{}^n=\frac{Z}{A}\frac{m}{M}\mathfrak{R}\equiv g_r{}^n\beta\mathfrak{R}. \quad (16)$$

Again, the general asymmetric top has been treated by Eshbach and Strandberg.[8] If we combine this with the electronic rotation-induced moment $-\beta\mathbf{L}_r=g_r{}^e\beta\mathfrak{R}$, we have a total rotational moment

$$\mathfrak{y}_r=\mathfrak{y}_r{}^n+\mathfrak{y}_r{}^e=(g_r{}^n+g_r{}^e)\beta\mathfrak{R}=g_r\beta\mathfrak{R}. \quad (17)$$

We now compute the energy contributed by the interaction of this total rotational moment with the external field. It is

$$\begin{aligned}\mathfrak{H}_{mr}&=-g_r\beta H\mathfrak{R}_Z\\&=-g_r\beta H(M-S_Z).\end{aligned} \quad (18)$$

M is, of course, a known good quantum number. For this small correction term we need only to use the diagonal value of S_Z, $\langle S_Z\rangle$, in the representation in which the sum of $\mathfrak{H}_0$ and the interaction of the spin moment with the external field is diagonal. We note that the eigenenergy is given by the diagonal elements of $\mathfrak{H}_0$ and S_Z in this representation as

$$E_M=\langle\mathfrak{H}_0\rangle-g_s{}^e\beta H\langle S_Z\rangle_M.$$

Thus, to first order,

$$\langle S_Z\rangle_M=-(1/g_s{}^e\beta)(\partial E/\partial H)_M. \quad (19)$$

The total first-order energy shift caused by the rotational moment is then

$$\langle\mathfrak{H}_{mr}\rangle_M=-g_r\beta H[M+(1/g_s{}^e\beta)(\partial E/\partial H)_M]. \quad (20)$$

Accordingly, the change in frequency for a transition from $M\rightarrow M+\Delta M$ is

$$\begin{aligned}\Delta\nu_r&=\langle\mathfrak{H}_{mr}\rangle_{M+\Delta M}-\langle\mathfrak{H}_{mr}\rangle_M\\&=-g_r\beta H[\Delta M+(1/g_s{}^e\beta)(d\nu/dh)],\end{aligned} \quad (21)$$

where $d\nu/dH=d(E_{M+\Delta M}-E_M)/dH$ is known from previous calculations (Eq. 7). The corresponding change in H required to maintain the fixed experimental resonance frequency is

$$\frac{\Delta H_r}{H}=\frac{g_r}{g_s{}^e}\left[\frac{g_s{}^e\beta\Delta M}{(d\nu/dH)}+1\right]. \quad (22)$$

Let us now take account of the energy of the spin-orbit induced orbital angular momentum in (15). From that equation

$$(JM\Sigma|\mathfrak{H}_{ml}|J'M\Sigma\pm1) =-g_l{}^e\beta H(JM\Sigma|S_Z|J'M\Sigma\pm1). \quad (23)$$

All other elements vanish. This clearly has a different form from the rotational interaction (18) or from the principal spin interaction $\mathfrak{H}_{ms}$. Thus all three will be experimentally separable. The first step in evaluating the contribution of (23) to the energy is to find the transformed elements in the basis which diagonalizes the field-free Hamiltonian $\mathfrak{H}_0$. This is done by using the transformation matrices T_J in the method of TSI Eq. (59). However, the results differ somewhat from TSI Eq. (60) since the $(\Sigma|\mathfrak{H}_{ml}|\Sigma)$ elements vanish. This transformed matrix $(KJM|\mathfrak{H}_{ml}|K'J'M)$ has elements $K'=K$, $K\pm2$ and $J'=J$, $J\pm1$. For the reasons given in section I-B, we may neglect all except $K'=K$ elements. These are written as $(J|\mathfrak{H}_{ml}|J')$ in the following:

$$\begin{aligned}\mathfrak{H}_{11}&=(K-1|\mathfrak{H}_{ml}|K-1)\\&=-g_l{}^e\beta H(-4a_{K-1}c_{K-1}M)[K(K-1)]^{-\frac{1}{2}},\\\mathfrak{H}_{22}&=(K|\mathfrak{H}_{ml}|K)=0=\mathfrak{H}_{13}=(K-1|\mathfrak{H}_{ml}|K+1),\\\mathfrak{H}_{33}&=(K+1|\mathfrak{H}_{ml}|K+1)\\&=-g_l{}^e\beta H(4a_{K+1}c_{K+1}M)/[(K+1)(K+2)]^{\frac{1}{2}},\\\mathfrak{H}_{12}&=(K-1|\mathfrak{H}_{ml}|K)\\&=-g_l{}^e\beta H\left[\frac{2(K+1)(K^2-M^2)}{K(4K^2-1)}\right]^{\frac{1}{2}}a_{K-1},\\\mathfrak{H}_{23}&=(K|\mathfrak{H}_{ml}|K+1)\\&=-g_l{}^e\beta H\left\{\frac{2K[(K+1)^2-M^2]}{(K+1)[4(K+1)^2-1]}\right\}^{\frac{1}{2}}c_{K+1},\end{aligned} \quad (24)$$

with the special case

$$(1,0,0|\mathfrak{H}_{ml}|1,1,0)=+g_l{}^e\beta H[\tfrac{2}{3}(1-M^2)]^{\frac{1}{2}}.$$

In these, a_J and c_J are the transformation elements of T_J given in Table V of TSI. They are both approximately $\frac{1}{2}$ for all J.

From these elements we may note that the magnitude of the total g-factors (diagonal matrix elements) of the $J=K\pm1$ levels are increased by (roughly) the fraction $g_l{}^e/g_s{}^e$, whereas those of the $J=K$ levels are unchanged. The off-diagonal elements are also increased, but in a different ratio. From these observations it is clear that if $g_l{}^e/g_s{}^e$ is positive (as it turns out to be), this inter-

[10] It might appear anomalous that this argument does not also apply to eliminate $(\Sigma|\Sigma)$ elements of $\mathfrak{R}_Z$. The reason is that Φ and $\mathfrak{R}$ both operate in the relative coordinate domain, making $\Phi_{Z_0}\mathfrak{R}_0$ a true matrix produce in which $(\Sigma|\Sigma)$ elements are generated from the $(\Sigma|\Sigma\pm1)(\Sigma\pm1|\Sigma)$ elements. Since S_0 operates only on internal coordinates, in the case of S we have a simple product and no such elements can be generated.

action will tend to shift the resonance to lower fields. However, to investigate the effect rigorously we must transform $(J|\mathcal{H}_{ml}|J')$ to the basis which diagonalizes $\mathcal{H}_{ms}+\mathcal{H}_0$. This is done with the transformation U given in II-B. The result is

$$(\tau|\mathcal{H}_{ml}|\tau)=(U^{-1}\mathcal{H}_{ml}U)_{\tau\tau}$$
$$=U_{1\tau}{}^2\mathcal{H}_{11}+2U_{1\tau}U_{2\tau}\mathcal{H}_{12}$$
$$+2U_{2\tau}U_{3\tau}\mathcal{H}_{23}+U_{3\tau}{}^2\mathcal{H}_{33}. \quad (25)$$

The shift in the calculated magnetic field to maintain the same resonant frequency is then

$$\Delta H_l=-(d\nu/dH)^{-1}[(\tau'|\mathcal{H}_{ml}|\tau')-(\tau|\mathcal{H}_{ml}|\tau)]. \quad (26)$$

In view of the difficulty of making these corrections, they have only been computed for 27 examples. These results are tabulated in Tables I and III. Clearly the agreement with experiment is satisfactory.

III. COMPARISON WITH EXPERIMENT

A. Experimental Method

Since the apparatus used will be described more fully elsewhere, only a brief sketch is given here. The microwave arrangement uses a Pound-Zaffarano[11] feedback circuit to stabilize the klystron frequency to the resonant frequency of the cavity containing the oxygen gas sample. This cavity is situated between the poles of a magnet the field of which is monitored by a flip coil. This flip-coil voltage is compared with a controllable fraction of the output of a small reference generator driven by the same shaft. The error signal is used in a feedback circuit to stabilize the field. The field is then slowly swept by using a geared down synchronous motor to vary the helipot which controls the comparison voltage. The stability is within a fraction of a gauss.

Upon this slowly sweeping field is superposed a 50-cps modulation, adjustable from 0 gauss to 80 gauss, peak to peak. It is also feedback-stabilized to eliminate phase and amplitude shifts with changing dc fields and hence changing properties of the iron core. Provided the modulation amplitude is small compared to the linewidth, this will produce a 50-cps component proportional to $d\chi''/dH$ (the derivative of the imaginary part of the sysceptibility) in the power absorbed in the gas, and hence in the reflection or transmission coefficient of the cavity. This modulated microwave power is detected with a crystal (or bolometer). The resulting 50-cps signal is amplified in a low-noise amplifier and converted to dc in a phase-sensitive detector which uses a Brown converter as the synchronous device. The output is recorded on a strip chart recorder. A block diagram of the apparatus is given in Fig. 5. (The bolometer bridge is, of course, absent when a crystal detector is used. This was the case for all measurements except those of absolute intensity.)

[11] R. V. Pound, Rev. Sci. Instr. **17**, 490 (1946); F. P. Zaffarano and W. C. Galloway, Technical Report No. 31, Research Laboratory of Electronics, Massachusetts Institute of Technology, 1947 (unpublished).

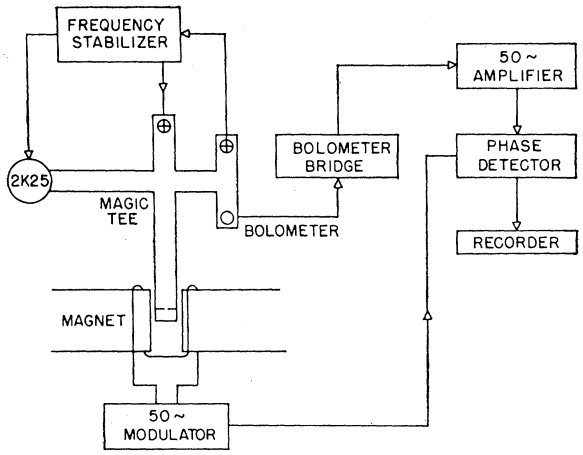

FIG. 5. Block diagram of the apparatus.

All precise measurements of the magnetic field are made by using proton resonance, the frequencies being measured with a BC-221 frequency meter accurate to ± 40 ppm by comparison with the M.I.T. frequency standard. The flip-coil arrangement gives readings accurate to a few gauss under normal operating conditions. Precise frequency measurements were made by beating the klystron frequency with harmonics of the M.I.T. frequency standard. Other frequency measurements were made with a calibrated wave meter.

The X-band measurements were made with the use of three different cavities. A TE_{011} cylindrical cavity with Q_0 of the order 35 000 was used for the highest sensitivity exploration. A much smaller TE_{011} rectangular cavity was used for the precise measurements to minimize errors caused by field inhomogeneity by allowing smaller pole separations. Finally, a TE_{111} cylindrical cavity was used in conjunction with special microwave plumbing to produce a circularly polarized radiation field in the cavity. This field is set up by exciting the two degenerate orthogonal modes 90° out of phase. This field configuration gives pure circularly polarized radiation only along the axis.[12] Averaging H^2 over the cavity, 52 percent is circular in one sense, 4 percent is circular in the other, and 44 percent is axial. Comparison of the spectra observed with the two senses of rotation relative to the static magnetic field unambiguously separates $\Delta M=\pm 1$, 0 transitions.

The rotational quantum number K of the states involved in a transition can be determined by a comparison of the relative signal strengths of various lines at room temperature and at 78°K if we note that the Boltzmann factor is given by $\exp[-BK(K+1)/kT]$ and if we assume that all line widths change in the same proportion. The well-known difficulty of making reproducible intensity measurements limits the accuracy of this determination to a mean deviation in K

[12] The fact that $\mathrm{div}\mathbf{H}=0$ makes this true for any configuration. With TM modes the energy would be *equally* divided between the two circular senses when averaged over the entire cavity.

TABLE I. Results on precisely measured X-band lines. The first column gives the observed magnetic field for resonance at the experimental frequency 9476.75 Mc/sec. The second column gives the resonance field calculated on the assumption that only the electronic spin moment is present. The spin-orbit correction ΔH_l was made by using the value $g_l^e=-0.00294$ determined by a least-squares fit. The correction for rotation-induced magnetic moment ΔH_r was made with $g_r=-0.25m/M$. The values of $d\nu/dH$ give the rate of change of the resonance frequency with field in the vicinity of the observed values H, ν. The calculated intensity factors listed in column 8 are the values of $4|(KJM|S_X|KJ'M')|^2\exp(-BK(K+1)/kT)$ at $T=300°$K. The experimental results are signal strengths at optimum modulation expressed in arbitrary units. Provided the frequency widths of all lines are essentially equal, the latter should be proportional to the calculated (integrated) intensities.

Experimental H (gauss)	Spin only, calculated H (gauss)	Corrections (gauss) ΔH_l	ΔH_r	Residual error (gauss)	(Mc/sec)	K	Transition J	M	$d\nu/dH$ (Mc/gauss)	Calculated intensity	Experimental signal strength
1402.1	1404.2					3	2→4	2→3	3.88		0.003
2342.4	2345.1					3	2→4	1→2	2.36		0.031
3552.8	3558.5					3	4→2	−3→−2	3.73		0.041
4155.0						5	6→4	−3→−2		0.135	0.12
4502.0						7	8→6	−3→−2			0.14
5158.0	5165.0					3	4→2	−1→−2	2.70		0.043
5264.4	5271.2	−8.1	1.1	−0.2	−0.3	3	2→4	1→0	1.33	0.034	0.024
5353.2	5360.4					5	4→6	1→2	1.84		0.37
5583.8	5586.4	−2.2	−0.1	0.3	0.5	1	1	−1→0	1.96	0.741	0.78
5768.5	5777.3	−8.5	−0.4	−0.1	−0.1	3	2→4	0→1	1.33	0.404	0.48
5977.8	5986.0	−8.3	−0.1	−0.2	−0.5	3	4→2	−2→−1	2.30	0.425	0.48
5999.3	6006.8	−8.0	1.0	0.5	0.9	5	6→4	−1→−2	1.88	0.060	0.034
6087.5	6094.7	−7.0	−0.2	0.0	0.0	1	2	1→2	1.74	1.21	1.34
6509.3	6517.7	−8.2	−0.4	−0.2	−0.4	5	6→4	−2→−1	1.74	0.545	0.57
6684.1	6692.4					7	8→6	−2→−1	1.52		0.55
6710.2	6718.6	−7.7	−0.6	0.1	0.1	1	2	0→1	1.42	1.50	1.45
7019.6	7029.2					11	10→12	3→4	2.14		0.21
7063.8	7072.9					9	8→10	2→3	2.01		0.26
7254.3	7262.9	−8.8	−0.5	−0.7	−0.9	1	2	−1→0	1.33	1.24	1.15
7354.9						7	6→8	1→2			0.78
7513.3	7502.9	−9.0	1.3	−0.1	−0.1	3	2	0→−1	1.77	0.351	0.31
7885.9	7892.9					5	4→6	1→0	1.72		0.26
8026.9	8036.8					13	12→14	3→4	2.10		0.36
8097.0	8106.1					5	4→6	0→1	1.72		1.15
8266.0	8271.9	−7.7	1.5	−0.3	−0.5	5	4	0→−1	1.76	0.285	0.43
8575.2	8582.6	−7.3	−0.4	−0.3	−0.6	3	4	−1→0	1.68	1.39	1.36
8639.3						7	8→6	−1→0			1.03
8704.8	8711.3					7	6	1→0	1.80		0.20
8729.4	8737.4	−7.0	−0.4	0.6	1.0	5	6	−1→0	1.73	1.26	1.24
8813.8	8821.7					7	8	0→1	1.82		1.11
8965.9	8972.6					9	8	1→0	1.80		0.092
9001.6	9009.8					11	12	0→1	1.72		0.61
9030.6	9038.2					9	10	0→1	1.81		0.84
9604.2	9618.0	−13.2	−0.7	−0.1	−0.1	3	4	3→4	1.30	0.859	0.84
10450±3						3	3	−3→−2		0.542	0.43
10749±3	10739.5	15.8	−3.5	2.8	1.3	1	1	0→1	0.483	0.241	0.20

from the true value of roughly 0.8. Since only odd integral values of K are allowed, this still gives a very useful restriction.

The S-band measurements were made with a TM_{010} cylindrical transmission cavity fed through $\frac{7}{8}$-inch coaxial line. In the Pound-Zaffarano[11] circuit a hybrid ring ("rat race") was used in place of the magic Tee used with the X-band wave-guide arrangement.

B. Results

Table I shows the results of the precise measurements and calculations for 36 X-band lines. The experimental field values should be accurate within roughly ±60 ppm. (The last two readings at highest fields had to be made with the flip coil since the field exceeded the range of our proton probe.) In the second column are given the values of H for resonance if only $\mathcal{H}_{ms}$ were effective. The next two columns give the corrections ΔH_l and ΔH_r calculated with (22) and (26). In making the corrections there are two parameters, g_r and g_l^e. These were fitted by least squares (omitting the inaccurate high field line) with the results that $g_r=-(1.42\pm0.22)\times10^{-4}$ and $g_l^e=-(2.94\pm0.05)\times10^{-3}$. The residual errors are tabulated both in field and frequency units. These are of course related by the $d\nu/dH$ factor tabulated in a later column. The agreement is well within the accuracy of the calculation and measurement of H.

Since the accurate calculation of even the uncorrected H is very tedious, it was desirable to try to identify as many of the other observed lines as possible by other means. In Table II we list the positions of 84 additional lines (at X band, but at 9430 Mc/sec rather than the 9476.75 Mc/sec of Table I). For each of them we list the K determined from the temperature dependence of the relative intensity and the ΔM determined by use of circular polarization. When these data in conjunction with the graphical plots of $E(H)$ mentioned in Sec. I permitted a reasonably secure identification, the com-

TABLE II. Survey of other X-band lines at 9430 Mc/sec. The accuracy of H is roughly ± 0.05 percent unless stated to the contrary. K was determined from the temperature dependence of the intensity. ΔM was determined by use of circular polarization. Then an attempt was made to identify lines completely by using a graphical plot of $E(H)$. If this failed, ΔM was recorded as (+) or (−) according to whether $\Delta M = +1$ or -1. The signal strength has the same scale factor as in the table of precisely measured lines.

Experimental H (gauss)	Transition K	J	M	Signal strength
1914	5	4→6	4→5	0.006
2005	7	8→6	−6→−5	0.006
2059	9	10→8	−6→−5	0.012
2210	3	2→4	2→1	0.004
2215	5	6→4	−5→−4	0.010
2465	5	4→6	3→4	0.019
2917	5	6→4	−4→−3	0.032
3141	11		(+)	0.034
3177	7	8→6	−4→−3	0.021
3194	7	6→8	4→5	0.065
3269	9	10→8	−4→−3	0.059
3418	5	4→6	2→3	0.069
3687	≤9		(−)	≤0.01
3715	11−13		(+)	0.031
3759	9		(+)	0.051
4048	7	6→8	3→4	0.082
4192	13		(+)	0.030
4264	9−11		(+)	0.050
4347	11	12→10	−3→−2	0.072
4541	9	10→8	−3→−2	0.11
4645	≥13		(+)	0.029
4725	13		(+)	0.052
4901	≥13		(+)	0.052
4978	11		(+)	0.099
5063	≥13		(+)	0.035
5370	≥11		(+)	0.075
5427	7	6→8	2→3	0.315
5638	9	8→10	3→4	0.34
5746			(+)	0.038
5891	11	10→12	4→5	0.16
6100	11	12→10	−2→−1	0.025
6165	13		(+)	0.13
6255	11		(+)	0.28
6328	7	8→6	−1→−2	0.080
6445	15		(+)	0.113
6558	9	10→8	−2→−1	0.39
6724	≥13		(+)	0.050
7018	≥13		(−)	0.126
7076	≤11		(+)	<0.06
7093	9	8→10	3→2	0.06
7395	≥15		(+)	0.097
7541	≥15		(+)	0.031
7560	13	14→12	0→−1	0.031
7588	≥15		(+)	0.055
7649	13	14→12	−1→0	0.27
7871			(+)	0.10
7969	11	12→10	0→−1	0.072
7999			(+)	<0.06
8089	11	10→12	2→3	0.40
8120	11	12→10	−1→0	0.47
8163	15		(+)	0.030
8178	11	10→12	3→2	0.109
8303	15		(+)	0.036
8359	7−9		(−)	0.19
8371			(+)	<0.03
8391	9	8→10?	1→2?	0.63
8403	9	10→8?	−1→0?	0.76
8424			(+)	0.18
8652	≥15		(+)	0.11
8663			(+)	0.02
8671	≥13		(+)	0.16
8739	13	12	1→0	<0.04
8753	13	12→14	2→3	0.21
8777	13	14	0→1	0.24
8813			(+)	0.22
8833	11	10→12	2→1	0.011
8841	13	12→14	2→3	0.011
8900	11	10→12	1→2	0.67
8919	11		(−)	0.070
8934	11	10	1→0	0.042
9017			(+)	0.11
9044	15		(+)	0.19
9052	≥15		(+)	0.14
9074	15		(+)	0.18
9087	13	12→14	1→2	0.43
9103	13−15		(−)	0.06
9135	≥15		(+)	0.06
9150	≥15		(+)	0.16
9200	≥15		(+)	0.08
9238	≥15		(+)	0.06
11390±50				
11990±50				
12090±50				
12870±50				

plete specification of the transition is given. In this manner, an additional 37 lines were identified.

We note that a majority of the transitions are ones in which J changes by ± 2. These are allowed in the presence of the magnetic field, and theoretical intensities will be calculated in a subsequent section. Henry's[4] failure to consider the possibility of transitions of this sort accounts for his ability to identify only 6 lines of the total of 41 observed by Beringer and Castle.[13] The superior sensitivity of our sweep technique to the point-by-point technique of Beringer and Castle is demonstrated by our ability to measure 120 lines in the spectrum. The weakest observable lines are over a hundredfold weaker than the strongest lines of the spectrum at room temperature, and the range is 1000:1 at 78°K.

In Table III are listed the results of exact calculations for 34 S-band (2987 Mc/sec) lines and the corresponding experimental values. This table corresponds to the X-band results in Table I. Because of the uncertainty in the magnetic field over the large S-band cavity, these results are not as reliable as the X-band data. However, the magnitudes of the ΔH_r corrections are enough larger to provide some additional check on the choice of g_r. To give somewhat better agreement here, the value chosen was shifted from $-(1.42\pm 0.22)\times 10^{-4}$ to $-(1.35\pm 0.30)\times 10^{-4}$. This of course leaves the X-band agreement essentially unchanged.

Table IV lists the positions and signal amplitudes of 43 more S-band lines. Since neither K nor ΔM was determined experimentally, it was impossible to identify any of these from the $E(H)$ curves.

IV. DISCUSSION OF RESULTS

In Table V we collect parameters of the oxygen molecule which have become known or have been made more precise as a result of the work described in this

[13] R. Beringer and J. G. Castle, Jr., Phys. Rev. **81**, 82 (1951).

TABLE III. Identified lines of the S-band spectrum. The first column gives the observed magnetic field for resonance at the experimental frequency of 2987.0 Mc/sec. Limits of error are estimated to be ±0.06 percent. The other columns have the same significance as in the X-band table. The "signal amplitudes" are simply proportional to the deflections in a sweep made with constant amplitude magnetic field modulation.

Experimental H (gauss)	Spin only calculated H (gauss)	Corrections (gauss) ΔH_l	ΔH_r	Residual error (gauss)	(Mc/sec)	K	Transition J	M	$d\nu/dH$ (Mc/gauss)	Relative signal amplitude
1977.6	1977.9	−0.4	−0.1	−0.2	−0.3	1	1	−1→0	1.62	0.4
2091.0	2093.5	−2.4	−0.1	0.0	0.0	1	2	1→2	1.50	0.8
2162.3	2165.3	−2.6	−0.1	0.3	0.4	1	2	0→1	1.40	1.0
2239.1	2241.7	−2.8	−0.2	−0.4	−0.5	1	2	−1→0	1.31	1.0
2333.3	2336.8	−3.1	−0.2	0.2	0.2	1	2	−2→−1	1.20	0.3
2343	2348.5					1	1	0→1	1.14	0.3
2652	2651.8					3	4→2	−1→−2	2.20	0.2
2887	2889.7					3	2	0→−1	0.92	0.2
3039	3040.5					3	4→2	−2→−1	2.06	0.3
3372	3376.0					3	2	−1→−2	1.01	0.3
3633	3638.7	−8.1	1.2	−1.2	−0.8	3	2	1→0	0.68	0.2
3701	3703.6	−3.4	−0.5	−1.3	−1.2	3	4	−1→0	0.90	0.6
3751	3755.6					3	4	3→4	0.90	0.4
3854	3857.6	−4.4	0.9	0.1	0.1	5	4	0→−1	1.14	0.3
3945	3950.9	−4.9	−0.6	0.4	0.3	3	4	2→3	0.81	0.5
4167	4173.8					3	4	1→2	0.71	0.2
4218	4222.9					5	6	−1→0	1.06	0.3
4379	4383.9					7	6	1→0	1.15	0.1
4613	4620.0					3	4	0→1	0.52	0.3
4681	4683.9					5	4	−3→−4	0.71	0.3
5030	5043.8					3	4	−3→−2	0.49	0.4
5066	5075.1					5	4	−2→−3	0.58	0.3
5146	5155.3					3	4	−4→−3	0.48	0.2
5177	5183.8					5	6	5→6	0.70	0.3
5455	5472.5					3	4	−2→−1	0.42	0.1
5482	5491.7					5	6	4→5	0.61	0.2
5827	5835.5					5	6	3→4	0.53	0.3
5965	5976.3	−12.8	3.1	1.6	0.6	5	4	−1→−2	0.39	0.2
6017	6026.4					7	6	−5→−6	0.58	0.1
6276	6286.1	−8.9	−2.1	−0.9	−0.4	5	6	2→3	0.44	0.4
7190	7196.1					9	8	−7→−8	0.52	0.1
7510	7520.4					9	10	9→10	0.55	0.1
8210	8217.1					11	10	−9→−10	0.48	0.1
9235	9248.1					9	10	6→7	0.33	0.3

paper and in TSI. The system of interrelations which enable these parameters to be determined from the experimental data and compared with the theory are discussed in this section.

A. Source of Results

Direct Experimental Results

The spin coupling constants $\lambda_{(0)}$, $\lambda_{(1)}$, λ_1, and μ were determined directly by fitting the field-free spectrum with the theoretical formulas derived in TSI. The quantities λ_e and λ_2 follow immediately from the theory presented there, and may be considered on firm ground. Similarly, g_r and $g_l{}^e$ were determined by fitting the microwave spectrum in the presence of a magnetic field, under the assumption that $g_s{}^e=-2.00229$. On these quantities the quoted errors are the expected standard errors in a least-squares fit.

Derived Results

To separate the various physical mechanisms contributing to the parameters, we use the assumption (discussed in TSI) that the spin-orbit coupling parameter A and the reciprocal moment of inertia B can be treated as constants in the sums of matrix components which enter in the theory. Denoting the common factor $\sum_n|(0|L_x|n)|^2/(E_n-E_0)$ by $L(L+1)/h\nu$, and taking $B=1.44$ cm^{-1}, one may readily deduce values for λ_e', λ_e'', μ', μ'', A, $L(L+1)/h\nu$, χ_{H-F}, and R_e (as corrected for electronic contributions to B) from the above direct experimental results. These results are also tabulated. The quoted errors reflect only the errors in the direct experimental results. No attempt has been made to allow for the error introduced by our theoretical assumption.

Calculated Results

Finally, we also list the values for λ_e', λ_1', μ', and χ_{dia} which were obtained by direct calculation, using Meckler's expression for the molecular oxygen wave function. The method of calculation of λ' and μ' is given in TSI. No limit of error was assigned to these quantities for lack of any sound manner of estimation.

B. Discussion of Individual Results

Rotational Moment

A key to unraveling the entire problem experimentally was the fact that our precise Zeeman-effect measurements and theory have allowed us to determine

the rotational g-factor g_r defined in Eq. (17). Admittedly, the measurement is not of high accuracy, since it is based on small shifts superposed on the enormously larger splittings caused by the full Bohr magnetons of electron spin moment. Still, there is enough data to give reasonable assurance.

The magnitude and even the sign of g_r are rather unexpected. It is well known that in H_2 the electrons make almost no contribution to g_r, leaving $g_r = +0.883m/M = 0.883g_r^n$.[14] As another example,[8] OCS has $g_r = -0.025m/M$. There appear to be no examples of so large a negative g-factor as the $-0.25m/M$ which we find in O_2 in any of the molecules previously studied.

It is of interest to compare the oxygen result with the resulting moment if the electronic charge cloud merely rotated rigidly with the nuclei. One can readily show that in this case, we have

$$g_r = g_r^n + g_r^e = \frac{Z}{A} - \frac{\sum_i \langle x_i^2 + z_i^2 \rangle}{A(R/2)^2}, \qquad (27)$$

where z is the internuclear axis and R is the internuclear distance. These one-electron averages $\langle x_i^2 + z_i^2 \rangle$ are readily carried out with the use of Meckler's molecular orbitals (MO's) made up of Gaussian atomic orbitals (AO's). A simple integration shows that these Gaussian AO's have a value of $\langle r^2 \rangle$ which agrees with that of the Hartree-Fock atomic wave function[15] within 10 percent. This indicates that for a calculation of this type Meckler's MO's should give reasonably close approximations to the true values. The results are given in Table VI for each orbital. If we assumed that the electrons in all orbitals moved rigidly with the molecule, the resultant g_r^e would be $-0.758m/M$, and g_r would be $-0.258m/M$. This only slightly exceeds the experimental value. The agreement would still be within the experimental error and the error due to the wave functions if one assumed that the eight inner $1s$ and $2s$ electrons moved with unhindered precession about their nuclei, simply cancelling nuclear charge, while the eight outer $2p$ electrons moved rigidly. This is a more reasonable semiclassical model, since it is the asphericity of the charge distribution which causes it to rotate with the molecule.[16]

Viewed in terms of the rigorous quantum-mechanical picture, the unusually large g_r^e is probably a result of the fact that p orbitals, which would tend to have larger angular momentum matrix elements than s orbitals, are prominent in oxygen. This effect might be anticipated[17] by noting that the atomic correspondence at large R is to atomic P states, whereas in H_2 it is to S-states.

[14] N. J. Harrick and N. F. Ramsey, Phys. Rev. **88**, 228 (1952).
[15] Hartree, Hartree, and Swirles, Trans. Roy. Soc. (London) **A238**, 229 (1939). A very useful analytic approximation is given by P. O. Löwdin, Phys. Rev. **90**, 120 (1953).
[16] G. C. Wick, Phys. Rev. **73**, 51 (1948).
[17] J. H. Van Vleck, *The Theory of Electric and Magnetic Susceptibilities* (Oxford University Press, London, 1932), Chap. X.

TABLE IV. Survey of other S-band lines. The first column gives the observed magnetic field for resonance at the experimental frequency of 2987.0 Mc/sec. The limit of error is estimated to be ±0.06 percent. The signal amplitude column has the same significance as in Table III.

Experimental H (gauss)	Signal amplitude
2493	0.1
2743	0.1
2826	0.05
3159	0.2
3187	0.08
3398	0.2
3423	0.3
3440	0.3
3529	0.2
3587	0.1
3608	0.15
3830	0.2
4086	0.08
4322	0.06
4339	0.06
4436	0.2
4456	0.08
4493	0.2
4522	0.35
4713	0.3
4761	0.2
4819	0.2
6421	0.15
6481	0.2
6827	0.3
6937	0.2
7047	0.15
7083	0.15
7281	0.3
7320	0.15
7748	0.1
7828	0.3
7987	0.1
8010	0.2
8318	0.1
8401	0.2
8450	0.1
8485	0.1
8576	0.15
8612	0.15
8750	0.15
8876	0.15
9090	0.15

Spin-Orbit Coupling

The other key in the solution was the experimental measurement of g_l^e. With $\sum_n |(0|L_x|n)|^2/(E_n - E_0)$ evaluated from g_r^e, this gives us the spin-orbit coupling parameter A, and hence the second-order spin-orbit contribution λ'' to the parameter λ. As is clear from the table, λ'' is less than 1 percent of λ. Thus, even if this evaluation of λ'' has a serious fractional error, we are still assured that the first-order spin-spin contribution, λ', is the overwhelming one. This makes λ_e' and λ_1' firmly known quantities the calculation of which would serve as a test for the quality of a proposed electronic wave function. Since the calculation of TSI gave only 60 percent of λ_e', it is clear that the Gaussian MO's are not too good an approximation (even when adjusted as described there). On the other hand, the calculated λ_1' is roughly 16 percent too high. This is really as good agreement as one could expect.

TABLE V. Parameters of the oxygen molecule as determined in this work. As explained in the text, the quoted errors are standard errors based on least-squares fits of the experimental data. They include no estimates of the theoretical errors in the assumed interrelations and thus are not necessarily limits of error.

Symbol	Explanation	Numerical value: Experimental	Calculated
$\lambda_{(0)}$	$\lambda_{\text{eff}}(v=0)$	59 501.57±0.15 Mc/sec	
$\lambda_{(1)}$	$\lambda_{\text{eff}}(v=1)$	59 730±40 Mc/sec	
λ_e	$\lambda_e'+\lambda_e''$	59 386±20 Mc/sec	
λ_e'	spin-spin part	58 920±60 Mc/sec	35 000 Mc/sec
λ_e''	$\frac{1}{2}\sum_n \frac{\lvert(n\lvert AL_x\rvert 0)\rvert^2}{E_n-E_0}$	465±50 Mc/sec	
λ_1	$[R(d\lambda/dR)]_e$	16 896±150 Mc/sec	
λ_1'	$[R(d\lambda'/dR)]_e$		19 600 Mc/sec
λ_2	$[\frac{1}{2}R^2d^2\lambda/dR^2]_e$	$(5\pm2)\times10^4$ Mc/sec	
μ	$\mu'+\mu''$	−252.67±0.05 Mc/sec	
μ'	spin-nuclear part	1±4 Mc/sec	10.0 Mc/sec
μ''	$4\,\text{Re}\sum_n \frac{(0\lvert AL_x\rvert n)(n\lvert BL_x\rvert 0)}{E_n-E_0}$	(−254±4) Mc/sec	
g_l^e	$2\,\text{Re}\sum_n \frac{(0\lvert L_x\rvert n)(n\lvert AL_x\rvert 0)}{E_n-E_0}$	$-(2.94\pm0.05)\times10^{-3}$	
g_r	$g_r^n+g_r^e$	$-(1.35\pm0.30)\times10^{-4}=-(0.25\pm0.05)m/M$	
g_r^n	$(Z/A)(m/M)$		$2.72\times10^{-4}=0.500m/M$
g_r^e	$-4\,\text{Re}\sum_n \frac{(0\lvert L_x\rvert n)(n\lvert BL_x\rvert 0)}{E_n-E_0}$	$-(4.1\pm0.3)\times10^{-4}=-(0.75\pm0.05)m/M$	
R_e		1.20741±0.00002A	
$\frac{L(L+1)}{h\nu}$	$\sum_n \frac{\lvert(0\lvert L_x\rvert n)\rvert^2}{E_n-E_0}$	$(7.1\pm0.5)\times10^{-5}/\text{cm}^{-1}$	
A	spin-orbit coupling parameter	$-(21\pm2)$ cm^{-1}	
χ_{dia}	$\frac{-N_0e^2}{6mc^2}\sum_i\langle r_i^2\rangle$		-29.5×10^{-6} cm^3/mole
χ_{H-F}	$\frac{4N_0\beta^2}{3}\sum_n \frac{\lvert(0\lvert L_x\rvert n)\rvert^2}{E_n-E_0}$	$(24.6\pm1.7)\times10^{-6}$ cm^3/mole	
χ_{orb}	$\chi_{\text{dia}}+\chi_{H-F}$	$-(4.9\pm1.7)\times10^{-6}$ cm^3/mole	
χ_{spin}	$2N_0(g_s^e)^2\beta^2/3kT$		$1.003/T$ cm^3/mole

From g_l^e we directly find μ'', using the relation $\mu''=2Bg_l^e$. This second-order interaction of the rotation-induced orbital angular momentum with the spin gives essentially the entire spin-rotation coupling constant μ, leaving 1±4 Mc/sec for the first order μ'. Direct calculation of μ' (see TSI) gave 10.0 Mc/sec, and appeared insensitive to detailed choice of wave function. Since the experimentally deduced value is the difference of two large numbers, this agreement is reasonably good. A more informative check is to compare μ'' computed as above with the value obtained by subtracting the reliably computed μ' from the experimental μ. These results check to within 3.5 percent. Since the standard deviation in the least-squares fit is only 1.7 percent, this indicates that an error of the order of 1 or 2 percent may be introduced in removing B from the summation and giving it its value in the ground electronic state. This is a reasonable magnitude of error

since a more detailed examination shows that the expected error is of the same order of magnitude as the effect of zero-point vibration, which is 0.6 percent in O_2. It does not seem possible to make any equally simple estimate of the error introduced by removing A from the sum of matrix elements, nor, lacking a reliable calculated value for λ', can we check it experimentally. The error is no doubt greater with A than with B, but our partial check is still encouraging.

Another viewpoint would be to assume from the start that $g_l^e=(\mu-\mu')/2B$. In this, B and μ are known from the field-free spectrum, and μ' is easily calculated to good accuracy. Thus g_l^e is determined *a priori*. Since the contributions of g_r to the spectrum are small and of a distinctive form they are easily eliminated. The only free parameter then left for the Zeeman spectrum is g_s^e, the electron spin g-factor. Our excellent agreement of theory and experiment then demonstrates that this has the theoretical value[18] -2.0023 with a precision of 60 ppm (parts per million). This precision is two orders of magnitude less than that obtained by Koenig, Prodell, and Kusch[19] with atomic hydrogen. It is also an order of magnitude less than that of Abragam and Van Vleck[20] in their interpretation of the data on the atomic oxygen Zeeman effect taken by Rawson and Beringer.[21] Nevertheless, it is a reassuring check that there is no unexpected difficulty in treating the case of two coupled spins in a molecular, as opposed to an atomic, environment.[22]

Susceptibilities

Starting with a general formula of Van Vleck,[17] the molar susceptibility of a diatomic molecule with electronic spin S but no diagonal orbital angular momentum is seen to be

$$\chi=\chi_{\text{spin}}+\chi_{H-F}+\chi_{\text{dia}}$$
$$=\frac{N_0(g_s^e)^2\beta^2S(S+1)}{3kT}+\frac{4N_0}{3}\beta^2\sum_n\frac{|(0|L_x|n)|^2}{E_n-E_0}-\frac{N_0e^2}{6mc^2}\sum_i\langle r_i^2\rangle. \quad (28)$$

Evidently the first term is dominant since $kT\ll(E_n-E_0)$ in most cases and the diamagnetic term is always small. It is still of some interest to know the magnitudes of the temperature-independent terms, however, in making detailed comparison of precise experimental data with the theory. The χ_{dia} is easily calculated from Meckler's wave function, and the expected accuracy is again moderately good because the function r^2 puts no particular weight on the detailed behavior near the nucleus. The results are given for each orbital in Table VI. The high-frequency paramagnetic contribution χ_{H-F} is evaluated by using the value for $L(L+1)/h\nu$ determined from g_r^e. These two contributions nearly cancel, the diamagnetic term slightly exceeding the paramagnetic one. This remainder provides a correction of 5×10^{-6} cm^3/mole to the spin susceptibility, which is 3.42×10^{-3} cm^3/mole at $T=20$°C. This correction is small compared to the spread in the experimentally obtained values, but might be useful in explaining small departures from Curie's law. Since it is definitely too small a correction to explain the deviation found by Woltjer, Coppoolse, and Weirsma,[17] that deviation must be ascribed to experimental error.

TABLE VI. Integrals over oxygen molecular orbitals. The occupation numbers apply to the lowest-energy configuration (Meckler's ϕ_c). R is the internuclear distance, z is the internuclear axis, and r is measured from the center of mass of the molecule.

Orbital	Meckler notation	Occupation number	$\frac{\langle x^2+z^2\rangle}{(R/2)^2}$	$\langle r^2\rangle\times10^{16}$ cm^2
$1s\ \sigma_g$	φ_s	2	1.02	0.375
$1s\ \sigma_u$	χ_s	2	1.02	0.375
$2s\ \sigma_g$	φ_σ	2	1.36	0.585
$2s\ \sigma_u$	χ_σ	2	1.69	0.710
$2p\ \sigma_g$	φ_0	2	1.96	0.800
$2p\ \sigma_u$	χ_0	0	2.62	1.038
$2p\ \pi_u^{\pm}$	$\varphi_\pm$	4	1.61	0.760
$2p\ \pi_g^{\pm}$	$\chi_\pm$	2	1.87	0.855

V. LINE INTENSITIES

A. Theory

It is easily verified that the $1/Q$ increment caused by absorption in a gas-filled cavity is equal to $4\pi\chi''$ or to c/ω times the absorption coefficient α of the gas for a plane wave of suitable polarization. Further, in these Zeeman-effect studies all degeneracies are lifted, so there is no summation over M states. The standard analysis[23] then yields

$$\left(\frac{1}{Q}\right)_{ij}=\frac{4\pi\omega N}{kT}|(\mu_r)_{ij}|^2\frac{\tau^{-1}}{(\omega-\omega_{ij})^2+\tau^{-2}}\frac{e^{-E_j/kT}}{\sum_n e^{-E_n/kT}}, \quad (29)$$

where $|(\mu_r)_{ij}|^2$ is the average squared matrix element of $g_s^e\beta S_r$ or $\langle|g_s^e\beta\mathbf{H}_{rf}\cdot\mathbf{S}_{ij}|^2\rangle/\langle H_{rf}^2\rangle$, S_r being the component of $\mathbf{S}$ along $\mathbf{H}_{rf}$. Also τ^{-1} is $2\pi\Delta\nu$, $\Delta\nu$ being the frequency half-width at half-power absorption. Eliminating N by using the ideal gas law, approximating the partition sum by its classical value[24] $3kT/2B$, and setting $\omega=\omega_{ij}$, we find the maximum absorption to be

$$\left(\frac{1}{Q}\right)_{ij}=\frac{32\pi}{3}\frac{B\beta^2\nu}{(\Delta\nu/P)}\frac{e^{-BK(K+1)/kT}}{(kT)^3}|(S_r)_{ij}|^2. \quad (30)$$

[18] R. Karplus and N. M. Kroll, Phys. Rev. **77**, 536 (1950).
[19] Koenig, Prodell, and Kusch, Phys. Rev. **88**, 191 (1952).
[20] A. Abragam and J. H. Van Vleck, Phys. Rev. **92**, 1448 (1953).
[21] E. B. Rawson and R. Beringer, Phys. Rev. **88**, 677 (1952).
[22] These orders of magnitude are indices of the increasing difficulty of the problem as one proceeds from the simplest atom to a more complex atom, and finally to a molecule. For a molecular problem, our agreement is quite satisfactory.
[23] J. H. Van Vleck and V. F. Weisskopf, Revs. Modern Phys. **17**, 227 (1945).
[24] J. C. Slater, *Introduction to Chemical Physics* (McGraw-Hill Book Company, Inc., New York, 1939), p. 139.

TABLE VII. Table of field-dependent transformations U_K.

K	J	M	H (kilogauss)	$U_{1\tau}$	$U_{2\tau}$	$U_{3\tau}$
1	1	−1	1.98	0.000	1.000	0.024
		−1	5.55	0.000	0.991	0.136
		0	1.98	−0.038	0.996	0.056
		0	5.55	−0.103	0.982	0.148
		0	10.7	−0.176	0.954	0.244
		1	10.7	0.000	0.974	0.230
1	2	±2	—	0.000	0.000	1.000
		±1	2.2	0.000	−0.054	0.997
		−1	7.2	0.000	−0.171	0.985
		−1	8.8	0.000	−0.204	0.977
		0	2.2	0.050	−0.062	0.995
		0	6.7	0.040	−0.171	0.984
		0	7.2	0.048	−0.178	0.983
		1	6.0	0.000	−0.146	0.990
		1	6.7	0.000	−0.159	0.986
3	2	−1	6.0	0.935	−0.122	−0.331
		−1	7.5	0.914	−0.152	−0.377
		0	3.7	0.973	−0.138	0.182
		0	5.6	0.920	−0.216	0.326
		0	7.5	0.862	−0.281	0.419
		0	8.5	0.832	−0.316	0.455
		1	3.7	0.992	−0.114	0.070
		1	5.2	0.981	−0.163	0.107
3	3	−3	10.4	0.000	0.985	0.166
		−2	10.4	0.315	0.927	0.198
3	4	−2	6.0	0.089	−0.155	0.984
		−1	3.6	0.378	−0.139	0.915
		−1	8.5	0.338	−0.286	0.895
		0	3.6	−0.186	−0.086	0.978
		0	5.2	−0.304	−0.087	0.924
		0	8.5	−0.498	−0.075	0.863
		1	5.6	−0.139	−0.143	0.980
		2	3.9	−0.041	−0.106	0.993
		3	3.9	0.000	−0.088	0.995
		3	9.3	0.000	−0.228	0.974
		4	9.3	0.000	0.000	1.000
5	4	−2	4.1	0.984	−0.120	−0.130
		−2	5.9	0.968	−0.163	−0.182
		−1	3.8	0.958	−0.093	−0.272
		−1	6.0	0.922	−0.123	−0.363
		−1	6.5	0.914	−0.128	−0.381
		−1	8.2	0.884	−0.140	−0.448
		0	3.8	0.834	−0.166	0.523
		0	8.2	0.726	−0.321	0.608
		0	9.1	0.711	−0.342	0.602
5	6	−3	4.1	0.059	−0.109	0.993
		−2	6.5	0.164	−0.197	0.966
		−1	5.9	0.328	−0.216	0.920
		−1	8.7	0.388	−0.305	0.872
		0	8.6	−0.634	−0.014	0.774
		0	9.1	−0.650	−0.014	0.759
		2	6.3	−0.162	−0.158	0.974
		3	6.3	−0.096	−0.168	0.981

Evidently lowering the temperature gives a rapid rise in intensity for the lower rotational levels. Since our experimental frequency is fixed by the cavity, ν is the same for all lines. Also, it is an experimental fact that in oxygen the normalized line breadth parameter $(\Delta\nu/P)$ at a given temperature has the same value for all lines within roughly ±10 percent. (Beringer and Castle's[13] anomalous results were caused by their incorrect use of ν/H rather than $d\nu/dH$ to convert their field widths to frequency widths.) Thus at a given temperature, the variations of intensity from line to line come almost entirely from the factor $|(S_r)_{ij}|^2\exp[-BK(K+1)/kT]$. Since the Boltzmann factor is readily calculated, we are left only with the task of computing the matrix elements.

To handle the general case, it is convenient to expand H_{rf} as

$$\mathbf{H}=\mathbf{H}^+\mathbf{u}_+ + H^-\mathbf{u}_- + H_Z\mathbf{u}_Z,$$

where

$$H^\pm=(H_X\mp iH_Y)/\sqrt{2} \tag{31}$$

and

$$\mathbf{u}_\pm=(\mathbf{u}_X\pm i\mathbf{u}_Y)/\sqrt{2}.$$

The $\mathbf{u}_X$ and $\mathbf{u}_Y$ are unit vectors in the X and Y directions. Then

$$\mathbf{H}\cdot\mathbf{S}_{ij}=H^+(S_+)_{ij}/\sqrt{2}+H^-(S_-)_{ij}/\sqrt{2}+H_Z(S_Z)_{ij}, \tag{32}$$

where $S_\pm$ are $S_X\pm iS_Y$. Since the selection rules on matrix elements of S_+, S_-, and S_Z are all different (ΔM being +1, −1, and 0, respectively), only one term on the right will contribute to $(S_r)_{ij}$ for a given ij transition. The S matrix elements will have coefficients f, depending on the rf field and sample configurations, which give the fraction of the stored energy active in inducing each particular type of transition. For example

$$|(S_r)_{ij}|^2=\frac{\int_{\text{sample}}|H^+|^2d\tau}{\int_{\text{cavity}}H^2d\tau}\frac{|(S_+)_{ij}|^2}{2}\equiv\frac{f_+|(S_+)_{ij}|^2}{2}. \tag{33}$$

Finally, we note that with cylindrical symmetry about the static field direction Z,

$$|(\tau M|S_\pm|\tau'M')|^2=4|(\tau M|S_X|\tau'M')|^2 \tag{34}$$

for elements which exist in the left member. This enables us to write, in general,

$$|(S_r)_{ij}|^2=2|(S_X)_{ij}|^2[f_+\delta(M_i,M_j+1)+f_-\delta(M_i,M_j-1)]+|(S_Z)_{ij}|^2f_0\delta(M_i,M_j). \tag{35}$$

For nonrotating radiation perpendicular to Z in a gas-filled cavity, $f_+=f_-=\frac{1}{2}$. For localized samples, these numbers would obviously be reduced by filling factors. With pure circularly polarized radiation, one of the $f_\pm$ would be unity, all other f's being zero. (Rotation is possible only when two degenerate modes are excited out of phase.)

The procedure for calculating the required matrix elements, starting from the simple elements of S_g

referred to the gyrating coordinates g, can be symbolized as

$$(S_F)_{ij}=(U^{-1}T^{-1}S_FTU)_{ij}$$
$$=[U^{-1}T^{-1}(\textstyle\sum_g \Phi_{Fg}S_g)TU]_{ij}. \quad (36)$$

In this equation, the Φ_{Fg} are the direction cosines between fixed and gyrating axes; T is the transformation between the Hund case (a) basis (in which $S_z=\Sigma$ is diagonal, and in which we express Φ_{Fg} and S_g) and the basis which diagonalizes the field-free Hamiltonian; U is the transformation between the latter basis and the true eigenfunctions in the presence of the field. The transformations T are derived and tabulated in TSI; U is derived in Sec. I-B of this paper, and a number of specific cases are listed in Table VII.

For $F=Z$, $(T^{-1}S_FT)$ has been carried out in TSI and the result appears, multiplied by $-g_s{}^e\beta H$, as the terms linear in H in (4) of this paper. As discussed in Sec. I-B, we neglect the part of U which is off-diagonal in K. The resulting transformed matrix elements $(S_Z)_{ij}$ are of the type $(KJM|S_Z|KJ'M)$. For transitions possible below 50 kMc/sec, $J'=J\pm2$. These would be forbidden in the absence of the magnetic field, but, as noted in Sec. I-B, J breaks down as an angular momentum quantum number with increasing field and is kept only as a convenient label. On the other hand, at high fields $\mathfrak{IC}_{ms}=-g_s{}^e\beta HS_Z$ is such an important part of the Hamiltonian that when the total Hamiltonian is diagonalized, S_Z is nearly diagonal also. Thus the $(J|J\pm2)$ elements of S_Z never get very large. Detailed calculation verifies this conclusion, all $\Delta M=0$ transitions having a calculated intensity less than one percent of that of the strong $\Delta M=\pm1$ transitions. The conclusion is further substantiated by the fact that $\Delta M=0$ lines were not observed experimentally even when a cavity mode was used in which f_0 was 0.44.

The transformations are carried out in exactly the same manner for S_X. We can carry them analytically to

$$2(KJM|T^{-1}(\textstyle\sum_g \Phi_{Xg}S_g)T|KJ'M-1)=$$

$$\begin{array}{c|ccc} & J'=K-1 & J'=K & J'=K+1 \\ J=K-1 & [K(K-1)-M(M-1)]^{\frac{1}{2}} \times g(K,K-1)/g_s{}^e & C_{K-1}[(K-M)(K-M+1)]^{\frac{1}{2}} & 0 \\ J=K & -C_{K-1}[(K+M)(K+M-1)]^{\frac{1}{2}} & [K(K+1)-M(M-1)]^{\frac{1}{2}} \times g(K,K)/g_s{}^e & B_{K+1}[(K-M+1)(K-M+2)]^{\frac{1}{2}} \\ J=K+1 & 0 & -B_{K+1}[(K+M)(K+M+1)]^{\frac{1}{2}} & [(K+1)(K+2)-M(M-1)]^{\frac{1}{2}} \times g(K,K+1)/g_s{}^e \end{array}. \quad (37)$$

In this, the C_{K-1}, B_{K+1}, and $g(K,J)$ are defined in Eq. (60) of TSI and listed in Table VIII of that paper. We note that since we are dealing with $(M|M-1)$ elements there is no symmetry of this matrix about the diagonal. Thus one must take extra care to read off the correct element. Inspection of this matrix shows that $\Delta J=\pm2$ transitions are forbidden between the field-free eigenfunctions which form the basis for (37). The $\Delta J=\pm1$ transitions contribute to the millimeter spectrum treated in TSI. The $\Delta J=0$ elements are all proportional to $[J(J+1)-M(M-1)]^{\frac{1}{2}}$, and their squares will give the allowed transition probabilities in very weak fields.

For the fields of interest in this experiment, however, the departure of U from a diagonal (unit) matrix are so large (i.e., the J's are so mixed) that it is essential that the transformation U be applied. When this is done, it turns out that $\Delta J=\pm2$ transitions have appreciable intensities even at a thousand gauss, and that their intensity is of the same order as that of the "allowed" lines for fields above roughly 6 kilogauss. Of course, the intensities of the "allowed" lines is also strongly modified by U.

B. Comparison with Experiment

In Table I we list the values of $4|(S_X)_{ij}|^2 \times\exp[-BK(K+1)/kT]$ evaluated at $T=300°$K for those lines for which the entire calculation indicated above was carried through. As remarked in connection with Eq. (30), these factors should be nearly proportional to the experimental signal strength. ["Signal strength" is defined as proportional to $(1/Q)_{ij}$. It differs from the (integrated) intensity by a factor of $(1/\Delta\nu)$.] Inspection of the last two columns of Table I shows that the proportionality holds to an average of roughly ±10 percent over a range of almost 100:1 in absolute value. This agreement is highly satisfactory in view of the difficulty of the measurement and in view of the approximation that $\Delta\nu$ is the same for all lines.

An attempt was made to check (30) more completely by measuring the absolute intensity. Inserting the numerical values for $T=300°$K, with $\nu=9400$ Mc/sec and $(\Delta\nu/P)=2$ Mc/sec-mm Hg, one finds

$$(1/Q)_{ij}=1.46\times10^{-7}|(S_X)_{ij}|^2 \times\exp[-0.0069K(K+1)] \times[f_+\delta(M_i,M_j+1)+f_-\delta(M_i,M_j-1)]. \quad (38)$$

For linear polarization and the strong $K=J=1$, $M=-1\rightarrow0$ line, this formula gives[25] 1.36×10^{-8}. This

[25] Beringer and Castle (see reference 13) quote a calculated $1/Q$ of 0.46×10^{-8} under these same conditions. The discrepancy apparently comes from their value of $\mathfrak{M}^2$ which is defined as $g^2(S_X{}^2+S_Y{}^2)=8|(S_X)_{ij}|^2$. They use $\mathfrak{M}^2=\frac{1}{2}$, which is the value

conveniently establishes the scale factor for Table I, and any other cases can be computed by proportionality.

To relate these predictions to experimental data, we note that the power reflection coefficient of a cavity at its resonant frequency is[26]

$$|r|^2=[(\xi-1)/(\xi+1)]^2, \tag{39}$$

where $\xi=Q_e/Q_0$, Q_e being the external Q and Q_0 the unloaded cavity Q. Thus

$$\Delta|r|^2=4\xi(\xi-1)(\xi+1)^{-3}Q_0(1/Q)_{ij}. \tag{40}$$

The coefficient in this equation has a broad maximum at the optimum operating point $\xi=2\pm\sqrt{3}$ where $|r|^2=\frac{1}{3}$ At that point

$$\Delta|r|^2=0.385Q_0(1/Q)_{ij}. \tag{41}$$

This change in reflection coefficient gives a proportional change in power at the bolometer detector, which gives rise to a proportional unbalance voltage in the bolometer bridge. Collecting all coefficients of proportionality for our apparatus, we find the open circuit bridge output to be

$$\epsilon_{\text{rms}}=6.0\times10^{-3}Q_0P_0(1/Q)_{ij}, \tag{42}$$

where P_0 is the power (in mw) reflected to the bolometer by a total reflection at the cavity under the operating conditions. This formula presumes optimum sinusoidal modulation of the field, in which case the 50-cps modulation component of $|r|^2$ has a peak amplitude of roughly 0.46 of the total change given by (41). The ϵ_{rms} is measured by comparison with a GR microvolter which is substituted with appropriate attention to impedance considerations.

The absolute intensities of several lines were measured at both room temperature and 78°K by this method. In all cases the experimental values of $(1/Q)_{ij}$ were approximately a factor of two too low. In view of the difficulty in measuring all of the parameters accurately, it is quite possible that this represents only an accumulation of small errors. This seems rather unlikely, however, because of the high stability of the results with respect to changed conditions. It is worth noting that Beringer and Castle found a measured $(1/Q)_{ij}$ for the $K=J=1$, $M=-1\rightarrow0$ line, mentioned above, of 1.39×10^{-9}, a factor of *ten* less than our calculated value. Thus our factor of two is tantalizing, but not too surprising.

The general theory given in Sec. V-A is profitably used in consideration of the experiments with circular polarization. With the TE_{111} cavity used, integration over the field configuration shows that for a purely (+) circular excitation at a hole in the center of one end, we have $f_+=0.68$, $f_-=0.06$, and $f_0=0.26$. Thus on interchanging the sense of rotation with respect to the static magnetic field, the signals on $\Delta M=\pm1$ transitions change by factors of 12 in opposite directions, whereas the $\Delta M=0$ transitions are unaffected. Experimentally, the change in the $\Delta M=\pm1$ transitions was very close to this theoretical limit for ideal adjustment. As remarked above, no $\Delta M=0$ transitions could be observed.

---

of $|(S_+)_{ij}|^2$ or $4|(S_X)_{ij}|^2$ evaluated before the transformation U is applied. The transformation U increases the result by a factor of 1.48 and if we also supply the factor of 2 which they omit, agreement with our value is obtained.

[26] J. C. Slater, Revs. Modern Phys. **18**, 487 (1946).